Diversity of Long Terminal Repeat Retrotransposon Genome Distribution in Natural Populations of the Wild Diploid Wheat *Aegilops speltoides*

Elena Hosid,* Leonid Brodsky,* Ruslan Kalendar,† Olga Raskina,* and Alexander Belyayev*,[1]
*Institute of Evolution, University of Haifa, Mount Carmel, 31905 Haifa, Israel and †Agrifood Research Finland/Institute of Biotechnology Plant Genomics Laboratory, Institute of Biotechnology, Viikki Biocenter, University of Helsinki, FIN-00014 Helsinki, Finland

ABSTRACT The environment can have a decisive influence on the structure of the genome, changing it in a certain direction. Therefore, the genomic distribution of environmentally sensitive transposable elements may vary measurably across a species area. In the present research, we aimed to detect and evaluate the level of LTR retrotransposon intraspecific variability in *Aegilops speltoides* ($2n = 2x = 14$), a wild cross-pollinated relative of cultivated wheat. The interretrotransposon amplified polymorphism (IRAP) protocol was applied to detect and evaluate the level of retrotransposon intraspecific variability in *Ae. speltoides* and closely related species. IRAP analysis revealed significant diversity in TE distribution. Various genotypes from the 13 explored populations significantly differ with respect to the patterns of the four explored LTR retrotransposons (*WIS2*, *Wilma*, *Daniela*, and *Fatima*). This diversity points to a constant ongoing process of LTR retrotransposon fraction restructuring in populations of *Ae. speltoides* throughout the species' range and within single populations in time. Maximum changes were recorded in genotypes from small stressed populations. Principal component analysis showed that the dynamics of the *Fatima* element significantly differ from those of *WIS2*, *Wilma*, and *Daniela*. In terms of relationships between *Sitopsis* species, IRAP analysis revealed a grouping with *Ae. sharonensis* and *Ae. longissima* forming a separate unit, *Ae. speltoides* appearing as a dispersed group, and *Ae. bicornis* being in an intermediate position. IRAP display data revealed dynamic changes in LTR retrotransposon fractions in the genome of *Ae. speltoides*. The process is permanent and population specific, ultimately leading to the separation of small stressed populations from the main group.

LARGE cereal genomes are known to consist of an extraordinary number of transposable elements, in particular, LTR retrotransposons, which are highly dynamic (Bennetzen 1996; Wicker *et al.* 2003). Recent studies have shown that LTR retrotransposons are often found in different densities or copy numbers among individuals of the same species (Baucom *et al.* 2009; Belyayev *et al.* 2010), and "bursts" of transposable elements (TEs) in several species of angiosperms over time have been recorded (Vitte and Panaud 2003; Tsukahara *et al.* 2009; Belyayev *et al.* 2010). Although there are several known cases of temporal retroelement copy-number change, the important question of the level of current TE intraspecific variability across the area occupied by a particular species is still unclear, especially for a species whose area is declining or shifting under the influence of climate change. It is possible that populations with enhanced TE activity are more likely to survive as new forms, or even new species, during environmental fluctuations due to the production of an extended number of genomic variants for natural selection (Grant 1981; Raskina *et al.* 2004a; Belyayev *et al.* 2010). This is one of the key problems in understanding the mechanisms of speciation because, in a certain sense, intraspecific genome diversification, particularly the genesis of differences across eco-geographical gradients, could be regarded as a speciation precursor.

Dobzhansky's central–marginal model (Da Cunha and Dobzhansky 1954) assumes that populations near the center of a species' range usually display high levels of genetic and phenotypic variation, while populations on the margin of the range are monomorphic (for review see Eckert *et al.* 2008).

doi: 10.1534/genetics.111.134643
Manuscript received September 13, 2011; accepted for publication October 25, 2011
Supporting information is available online at http://www.genetics.org/content/suppl/2011/10/31/genetics.111.134643.DC1.
[1]Corresponding author: Laboratory of Plant Molecular Cytogenetics, Institute of Evolution, University of Haifa, Mt. Carmel, 31905 Haifa, Israel. E-mail: belyayev@research.haifa.ac.il

Extrapolating the central–marginal model onto the TE fraction and given the fact that TEs are sensitive to changes in the external environment (Wessler 1996; Kashkush *et al.* 2003; Grandbastien *et al.* 2005; Ansari *et al.* 2007; Martienssen 2008), it is possible to speculate that the TE quantity and structural distribution across the genome may perceptibly vary between populations. Indeed, the environment can have a decisive influence on the structure of the genome, changing it in a certain direction that could be heritable (Martienssen 2008). This is especially true in times of rapid climatic change such as the current period of global warming, when the average temperature of the Earth's near-surface air and oceans is increasing (http://www.ipcc.ch). Any climate fluctuation causes the movement of plant zones and, consequently, the degradation of peripheral populations (Tchernov 1988; Hofreiter and Stewart 2009). Mesic plant species on the periphery of the distribution area, especially in the Eastern Mediterranean, due to its proximity to the Afro-Arabian desert domain, will be the first to suffer the impact of the current global warming (Kröpelin *et al.* 2008; Rebernig *et al.* 2010). Certainly, this could cause a reaction in plant organisms and may lead not only to their extinction or recession but also possibly to the formation of new drought-resistant forms (Raskina *et al.* 2004b). Moreover, in marginal populations where the influence of the ecologically intensive processes of raciation and speciation may take place, some models suggest that these populations play an important role in the maintenance and generation of biological diversity (Mayr 1963, 1970; Brussard 1984; Kirkpatrick and Barton 1997).

In the present research, we aimed to detect and evaluate the level of LTR retrotransposon intraspecific variability in *Aegilops speltoides* ($2n = 2x = 14$), a wild cross-pollinated relative of cultivated wheat. The interretrotransposon amplified polymorphism (IRAP) protocol (Kalendar and Schulman 2006), in which segments between two nearby retrotransposons or LTRs are amplified using outward-facing primers, was applied to determine the diversity of TE elements. We explore IRAP patterns from the Ty1-*copia* and Ty3-*gypsy* superfamilies (Kapitonov and Jurka 2008), which predominate in the repetitive fraction in *Ae. speltoides* (Belyayev *et al.* 2010).

Materials and Methods

Plant material and DNA extraction

Thirteen populations of *Ae. speltoides*, throughout the species distribution area, and three populations of related diploid S-genome species, *Ae. sharonensis*, *Ae. longissima*, and *Ae. bicornis* (195 plants totally), were selected for analysis. The geographical distribution of the explored populations is shown in Figure 1. In our experiments we used the continuous sampling, allowing estimation of the studied parameter across the entire species area. The abbreviation of the populations, their origin, and the number of analyzed genotypes are shown in Table 1. Sources of plant material and characteristics of *Ae. speltoides* populations are shown in supporting information, Table S1. Total DNA was extracted by the CTAB method (Kidwell and Osborn 1992). The purity and quality of the DNA were equivalent among all samples.

TE sequence sources and primer design

To determine the interpopulation diversity of four LTR retrotransposons (*WIS2*, *Wilma*, *Daniela*, and *Fatima*), IRAP analysis of the populations was performed, and the results were compared among themselves and with IRAP data from closely related species of section *Sitopsis*. This type of data provides insights into the dynamics of LTR retrotransposons in the genome of *Ae. speltoides* under changing environments. The sequences of transposable elements were taken from the TREP database (Table 2; http://wheat.pw.usda.gov/ggpages/ITMI/Repeats/index.shtml). Different LTRs of certain elements may vary in sequence at specific locations and may have point mutations, but there are places where polymorphism is reduced to a minimum. For each TE family, the sequence accessions were aligned, and the conservation was assessed with the multiple alignment procedure of MULTALIN (http://npsa-pbil.ibcp.fr/cgi-bin/npsa_automat.pl?page=/NPSA/npsa_multalinan.html). The conserved segments of the LTR or internal domain of the retrotransposons were used for the design of PCR primers, which was carried out with the program FastPCR (http://www.biocenter.helsinki.fi/bi/programs/fastpcr.htm). We designed several primer pairs for each of the repeated elements or TEs to compare the efficiency and reproducibility of amplification. None of the primer pairs chosen form dimers, and all showed high PCR efficiency. The chosen primers match motifs sufficiently conserved in the retrotransposons to allow amplification of almost all targets in the genome.

IRAP analysis

IRAP analysis was conducted according to Kalendar and Schulman (2006). Four additional informative primers were chosen (Table 3) and were labeled with fluorescent tags. The PCR was performed in a 20-μl reaction mixture containing 20 ng DNA, 1× PCR Y buffer [20 mM Tris-HCl (pH 8.55), 2 mM $MgCl_2$, 16 mM $(NH_4)_2SO_4$, and 0.01% Tween 20], 0.2 μM of each primer, 0.2 mM dNTPs, and 1 unite SAWADY Taq DNA polymerase (PEQLAB Biotechnologie, Erlangen, Germany). The PCR program consisted of (1) 1 cycle at 95° for 5 min; (2) 30 cycles at 95° for 30 sec and at 56°, 58°, or 60° (depending on the primer) for 1 min and at 72° for 30 sec; and (3) a final extension step of 72° for 5 min. Amplification was performed in a PTC-100 Programmable Thermal Controller (Applied Biosystems, Foster City, CA) in 0.2-ml tubes or in 96-well plates. Products were analyzed by gel capillary electrophoresis on an automated 3130xl genetic analyzer (Applied Biosystems) in polyacrylamide gels (Pop 7; Applied Biosystems), using the internal size standard *1200 liz* (Applied Biosystems) and standard running protocol *1200 long up*. The capillary gel electrophoresis

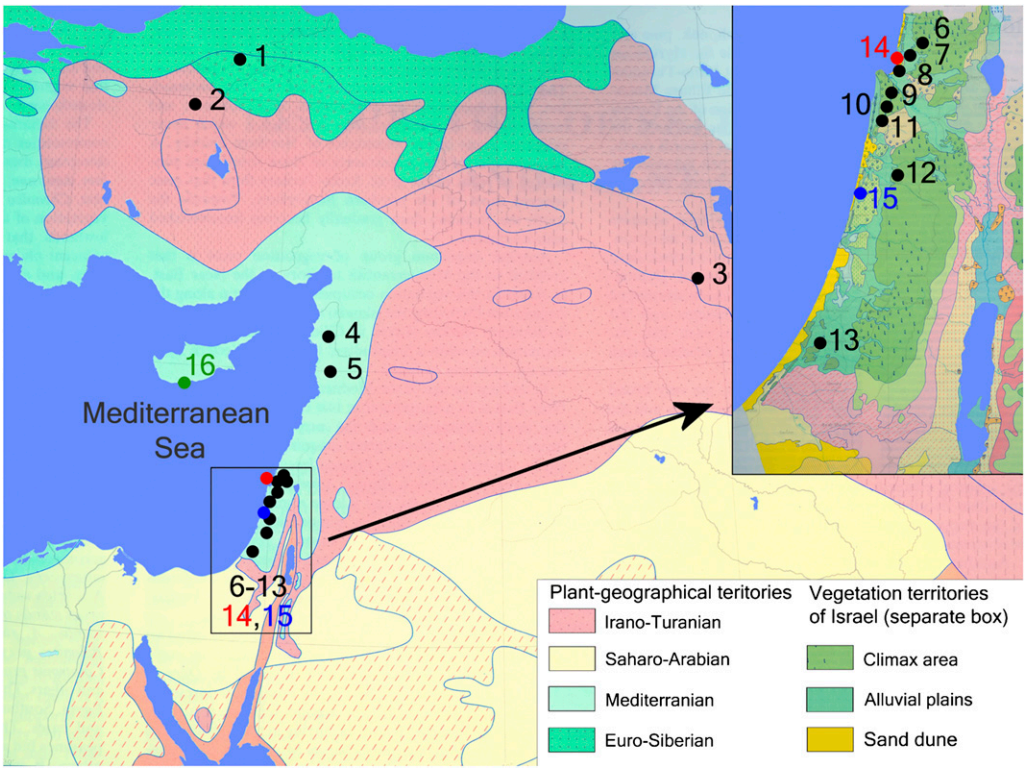

Figure 1 Geographical distribution of explored populations. Populations are numbered according to Table 1. *Ae. speltoides* populations are shaded in black, *Ae. sharonensis* in red, *Ae. longissima* in blue, and *Ae. bicornis* in green.

results were analyzed using *Gene Mapper* version 4.0 (Applied Biosystems) (Figure 2).

Data processing methods

The raw IRAP data for every genotype consisted of logarithms of peak areas across IRAP bands. The purpose of log transformation was to make the signal distribution of every genotype close to the Gaussian distribution. Then, all genotype log profiles were normalized by quantile normalization (Bolstad *et al.* 2003) to avoid an artificial deviation of some genotypes from their population pools due to a trend in signal measurements of the sample. In the first step of the analysis, the normalized data were studied by the singular value decomposition (SVD) version of principal component analysis (PCA) (Press *et al.* 2007) (Figure 3). For all four transposons, an obvious clustering of populations was observable. However, the first two components (PC1 and PC2) covered only 11–14% of the total data variance in each IRAP data set. To check how well the populations are separated in PCA spaces of higher dimensions, quadratic discriminant analysis (QDA) (R-package, CRAN; http://www.r-project.org) was performed with the populations as discriminating

Table 1 The accessions numbers and sources of plant material

No.	Species, genome	Abbreviation	Origin	No. genotypes analyzed
1	*Ae. speltoides*, SS	C	Cankiri, Turkey	6
2		An	Ankara,Turkey	4
3		Ar	Arbil, Iraq	2
4		TS-84	Latakia, Syria	1
5		Ta	Tartus, Syria	6
6		A	Achihood, Israel	12
7		E	En-Efek, Israel	2
8		Q	Kishon, Israel	36
9		T0, T2, T5	Technion 2, Israel[a]	16, 22, 13
10		R	Ramat Hanadiv, Israel	23
11		K, TS89	Katzir, Israel	27
12		TS43	Givat Koah, Israel	2
13		TS01	Ashkelon, Israel	4
14	*Ae. sharonensis*, $S^{sh}S^{sh}$	S	Kishon, Israel	10
15	*Ae. longissima*, $S^{l}S^{l}$	L	Wingate, Israel	8
16	*Ae. bicornis*, $S^{b}S^{b}$	TB	Cyprus	2

[a] For the Technion 2 population plants collected in three different years were analyzed: T0, collection of 2000; T2, collection of 2002; and T5, collection of 2005.

Table 2 Transposable element accessions

TE, superfamily	Accessions
WIS2, *Copia*	TREP1723, TREP1724, TREP839, TREP840, TREP841, TREP262, TREP1823, TREP1824, TREP1825, TREP1826, TREP818, TREP819, TREP1325, TREP1439, TREP1440, TREP1441, TREP1442, TREP1443, TREP10, TREP96,TREP105
Wilma, *Gypsy*	TREP842, TREP820, TREP821, TREP822, TREP1438, TREP2210
Daniela, *Gypsy*	TREP796, TREP1226, TREP2208, TREP231, TREP1408, TREP1228
Fatima, *Gypsy*	TREP827, TREP828, TREP252, TREP1229, TREP1230, TREP1804, TREP2209, TREP1231, TREP1232, TREP1306, TREP1413, TREP1414, TREP1415

classes (Figure 4). The QDA is applied to classification of the individual object of interest assuming that there are several populations of objects, to one of which the questionable object belongs, and also assuming that the intrapopulation distribution of objects could be approximated by multidimensional Gaussians. The QDA analysis is based on the hypothesis that the population-associated Gaussians mutually differ in their shapes (the covariation matrices of Gaussians differ both in their diagonal and in their nondiagonal elements). On the first step QDA approximates populations by Gaussians of most appropriate shape and detects the multidimensional subspaces that separate the populations. The following up classification of any individual object of interest is based on a separation of populations by these subspaces. In PCA spaces of three components, we estimated how many QDA misclassifications appear in each population. We also performed QDA for five components (data not shown), but the misclassification in the PCA-3 space was heavier and more informative because the space was more "narrow" (*i.e.*, of fewer dimensions). On the basis of the number of misclassifications and which populations are mutually confounded, one can evaluate an "IRAP distance" between populations or, in other words, detect the groups of similar populations.

Molecular cytogenetical retrotransposon display

The procedure of *in situ* hybridization retrotransposon display has previously been described (Belyayev *et al.* 2001). Degenerative oligonucleotide primers were used for PCR amplification of conserved reverse transcriptase regions present in the genomic DNA. The primers and PCR conditions used for the Ty1-*copia* elements have been previously described by VanderWiel *et al.* (1993); likewise, those for the Ty3-*gypsy* elements have been described by Purugganan and Wessler (1994). The gel-isolated amplification products of the RT domain of the two retroelements were labeled with biotin-16-dUTP (Roche) and used as probes for *in situ* hybridization experiments. Hybridization was carried out at 63° for 3 hr. Biotin was detected with fluorescein isothiocyanate (FITC)-conjugated avidin (Vector Laboratories, Burlingame, CA).

Table 3 Primers for IRAP analysis

Name	Sequence	TE, region
2106	taatttctgcaacgttccccaaca	*WIS2*, LTR
2108	agagccttctgctcctcgttgggt	*Wilma*, LTR
2109	tacccctactttagtacaccgaca	*Daniela*, LTR
2115	caagcttgccttccacgccaag	*Fatima*, LTR

Results

Defining populations

The importance of clearly defining normality/marginality of populations should be emphasized. The main criteria that we used for designating populations as marginal were as follows: (i) the position relative to the center of the species' range [the present-day center of the *Ae. speltoides* range is in the middle of the Fertile Crescent (Zohary *et al.* 1969; Kimber and Feldman 1987) and is limited to the approximate geographic coordinates 36°–38°N, 37°–41°E], (ii) population size (the area inhabited by small populations was <1000 m^2), (iii) the degree of population destruction (mainly due to human activity), (iv) local ecology (mainly abiotic components), and (v) elevation (optimum range from 100 to 1000 m above the sea level). The characteristics of the surveyed populations using the criteria listed above can be found in Table S1. We intended to explore three groups of populations that were clustered according to size and eco-geographical conditions: large populations with conducive environments [TS84 (Latakia, Syria), A (Achihood, Israel), R (Ramat Hanadiv, Israel), and K (Katzir, Israel)], small marginal populations [C (Cankiri, Turkey); An (Ankara, Turkey); Ar (Arbil, Iraq); Ta (Tartus, Syria); Q (Kishon, Israel); and T0, T2, and T5 (Technion 2, Israel)], and intermediate populations [E (En-Efek, Israel), TS43 (Givat Koah, Israel), and TS01 (Ashkelon, Israel)]. In our research, emphasis was given to small, marginal, stressed populations on the southern border of the species' range for several reasons: (i) long-term field observations have shown that modern climate change has led to the degradation of these populations, resulting in at least a threefold reduction in their size over the last decade; and (ii) our previous investigations have shown increased activity of TEs in the marginal populations (Raskina *et al.* 2004a; Belyayev *et al.* 2010).

IRAP analysis

IRAP is a novel method in which the insertion of a retrotransposon near another creates a new template for PCR amplification. The PCR products and, therefore, the fingerprint

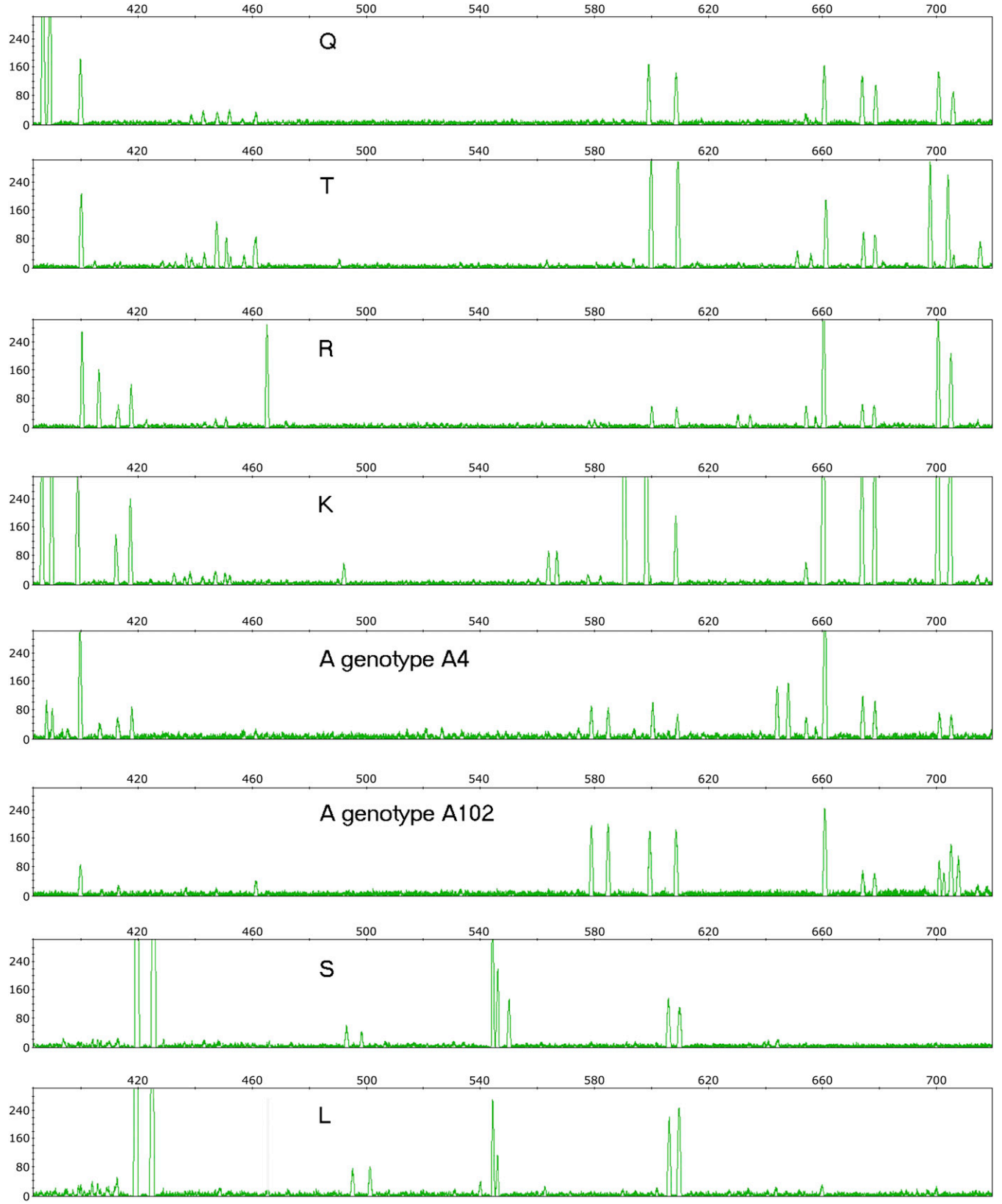

Figure 2 Example of interretrotransposon amplified polymorphism in the range from 400 to 720 bp for *Wilma* retrotransposons. Each peak indicates the presence of the amplified DNA fragment of a certain length. Abbreviations of populations are according to Table 1.

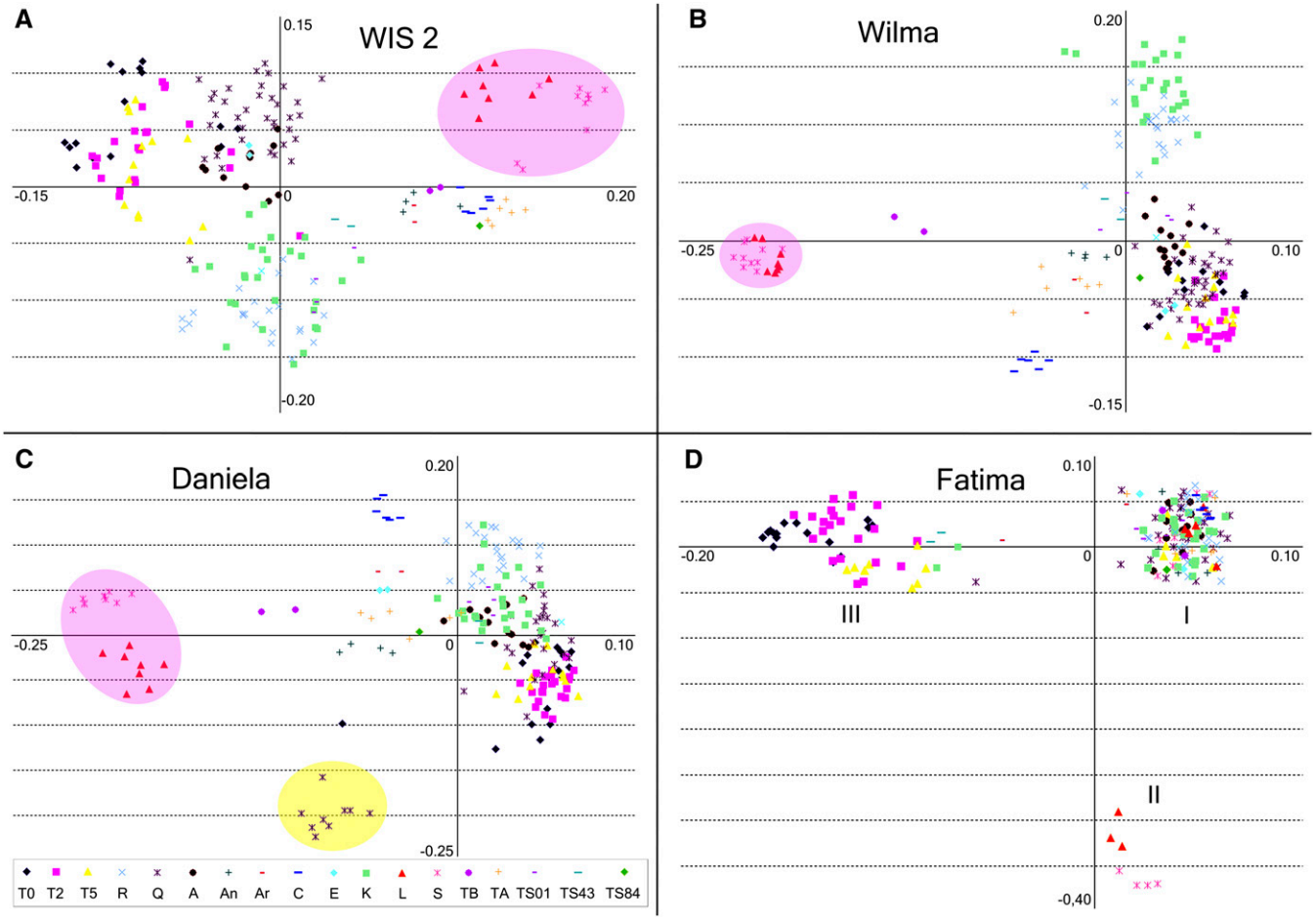

Figure 3 Distribution of populations in the space of the two first principal components. PC1 is located on *x*-axes, and PC2 is on *y*-axes. The raw data for the PCA analysis consist of the appearances of each IRAP band in the individual genotypes. The PCA algorithm was singular value decomposition (SVD). The obvious clustering of populations in the space of the first two PCs (11.4% of total variance) is clearly observed. (A) *WIS2* element IRAP pattern variability. (B) *Wilma* element IRAP pattern variability. (C) *Daniela* element IRAP pattern variability. Genotypes from the Kishon (Q) population with unusual IRAP patterns are shaded in yellow. (D) *Fatima* element IRAP pattern variability. Three groups are marked with Roman numerals. (A–C) *Ae. sharonensis* and *Ae. longissima* genotypes are shaded in pink.

patterns, result from amplification of hundreds to thousands of target sites in the genome (Kalendar and Schulman 2006). Polymorphisms consonant with large changes in TE chromosomal distribution would be expected. All IRAP primers produced multiple fragments from genomic DNA of all *Ae. speltoides*, *Ae. sharonensis*, *Ae. longissima*, and *Ae. bicornis* accessions (Figure 2 and Table S2). We took into account the fragments ranging from 250 to 1200 bp, which correspond to the maximum accuracy of the assay. The numbers of bands varied for different transposons and populations. *WIS2* retrotransposons produced the greatest number of bands, displaying between 41 [L (Wingate, Israel) and TS84 populations] and 159 (A population) bands with an average of 108 bands. *Wilma* elements produced between 50 (TS43) and 87 [TB (Cyprus)] bands with an average of 62 bands. *Daniela* elements produced between 32 [S (Kishon, Israel)] and 84 (T5) bands with an average of 77 bands. *Fatima* elements produced between 32 (K) and 53 (E) bands with an average of 44 bands.

Multivariate analyses

For statistical evaluation of the IRAP data, we used two types of analysis: PCA and QDA.

PCA analysis

The central idea of PCA is ". . . to reduce the dimensionality of a data set consisting of a large number of interrelated variables, while retaining as much as possible of the variation present in the data set. This is achieved by transforming to a new set of variables, the principal components (PCs), which are uncorrelated, and which are ordered so that the first few retain most of the variation present in all of the original variables" (Joliffe 2002, p. 1). We used PCA to project the populations onto a plane with minimal disturbances in distances between individual genotypes and to check visually how good the biologically defined populations are separated on the plane of the first two PCs. The data distribution in two-dimensional PCA

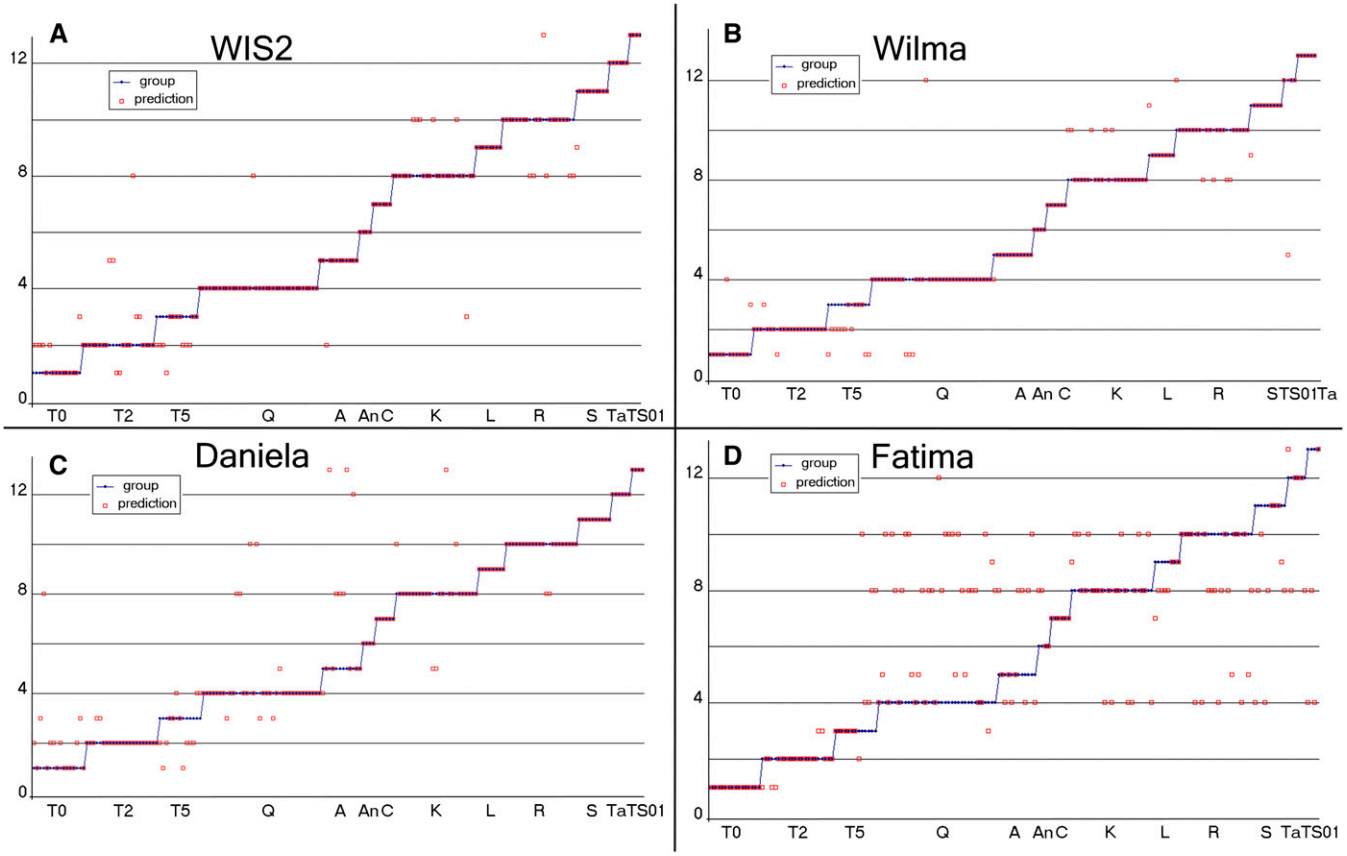

Figure 4 Prediction for 13 populations by QDA that is based on genotype values of the first three PCs (15% of total data variance). Populations are located on *x*-axes and clusters on *y*-axes. The blue dots depict classes of discrimination (*i.e.*, populations) for individual genotypes. The red circles depict what discrimination classes are predicted for individual genotypes by their QDA posterior probabilities. (A) QDA for *WIS2* retrotransposons. (B) QDA for *Wilma* retrotransposons. (C) QDA for *Daniela* retrotransposons. (D) QDA for *Fatima* retrotransposons.

spaces (Figure 3) visually demonstrates a clear separation of different populations for each of the explored LTR retrotransposons.

WIS2: Primers for *WIS2* retrotransposons produced a mostly dispersive picture (Figure 3A), although all genotypes in each population occupy sufficiently dense zones, and these zones overlap very often. *Ae. sharonensis* (S) and *Ae. longissima* (L) make up a separate group. However, *Ae. bicornis* (TB) joins the group of peripheral *Ae. speltoides* populations, which are intermediate between the two *Sitopsis* species and a majority of *Ae. speltoides* populations. Israeli populations of *Ae. speltoides* have specific *WIS2* retrotransposon distributions with a significant extent of variability. An analysis of plants collected in three different years in the Technion 2 population (T0, T2, and T5) showed clustering for the years 2000 and 2002 and overlapping with the following year (2005).

Wilma: IRAP analysis of the *Wilma* retrotransposon (Figure 3B) classified species in the best way; that is, *Ae. sharonensis* (S) and *Ae. longissima* (L) represent a separate compact group. *Ae. bicornis* (TB) takes an intermediate position between the two *Sitopsis* species and *Ae. speltoides*. The *Ae. speltoides* genotypes represent a dispersed group where the two biggest populations, K and R, grouped together and were distanced from the majority of the other populations. The northernmost peripheral population, C, is also separated.

Daniela: IRAP analysis of the *Daniela* retrotransposon (Figure 3C) was similar to that of *Wilma*, with a separate position for *Ae. sharonensis* (S) and *Ae. longissima* (L), an intermediate position for *Ae. bicornis* (TB), and a separate position for *Ae. speltoides*. The C population and several genotypes from the Q population (indicated by the yellow circle in Figure 3C) stood out substantially. The K and R populations composed a common core group with other populations.

Fatima: The IRAP pattern distribution of the *Fatima* retrotransposon differs significantly from those of the three other retroelements (Figure 3D). We observed complete dissolution of interpopulation and interspecific differences in the IRAP patterns. All genotypes were separated into three distinct groups. The largest group (group I in Figure 3D) includes the majority of populations throughout the *Ae. speltoides* distribution area, all genotypes of *Ae. bicornis* (TB), and several of the *Ae. sharonensis* (S) and *Ae. longissima* (L) genotypes. The second group (group II in Figure 3D) incorporates a few genotypes of *Ae. sharonensis* and *Ae. longissima*. The third

group (group III in Figure 3D) consists of the majority of genotypes of the Technion 2 population (T0, T2, and partially T5), one genotype from the Q population, one from TS01, two from TS43, and two from K.

QDA analysis

Statistically, a more accurate study by QDA (Figure 4) identifies differences in LTR retrotransposon-specific approximate IRAP distances between populations (namely, the structure of population clustering). The populations inside of each cluster are mutually misclassified by QDA. Each point represents a single genotype, and each line represents a single population. The QDA algorithm determines in which set (population) a genotype belongs on the basis of its IRAP pattern. If the genotype is similar to others of a given population, the QDA algorithm "puts" it into the same position as the population on the *y*-axis. If not, the genotype is positioned with respect to other populations that have a similar IRAP pattern while maintaining the genotype position on the *x*-axis. For example, in Figure 4A, five genotypes from the first population (T0) have IRAP patterns similar to the second population (T2) and one from the third population (T5). These misclassifications represent ~40% of the observed genotypes. However, 60% of the genotypes in the T0 population are homogeneous; *i.e.*, they form an individual "cloud". Thus, the QDA method allows for the evaluation of a population's homogeneity and separation. We applied QDA to classify all genotypes in all populations after approximating each population's distribution with Gaussian curves of population-specific shapes in the space of the first three principal components. The space of the first principal component was used in the QDA classification because all large populations are well separated in this space. These two types of analyses allowed us to evaluate the similarities and differences in the set of populations.

WIS2: QDA analysis showed that the number of misclassifications is significant (short IRAP distance) in two groups of populations: (1) Technion 2 (T0, T2, and T5) for all years collected (which was predictable, since it is the same population) and (2) K and R (Figure 4A). The predicted classes in each of these two population groups are not in good correspondence with the initial classes. It must be emphasized that Katzir and Ramat Hanadiv are the largest among all investigated natural populations with minimal destruction. The investigated *Sitopsis* species S, L, and TB showed no misclassifications.

Wilma: QDA analysis showed that the number of misclassifications for *Wilma* is the lowest of all the investigated elements. The same groups of populations were found as for *WIS2*.

Daniela: QDA analysis showed that the level of misclassification for *Daniela* is comparable with that for *WIS2* elements. Misclassifications were evenly distributed throughout populations and significant only in one group, which consists of the T0, T2, and T5 and Q populations.

Fatima: QDA analysis showed a significant level of misclassification across all populations and the investigated *Sitopsis* species, emphasizing the specific behavior of the *Fatima* element (Figure 4D). The most spread-out group is the Q population, which shows similarity with the rest of the *Ae. speltoides* populations and with *Ae. longissima* (L). All populations show the greatest similarity to the K population.

Summarizing the data from statistical analysis, it should be emphasized that there is a significant difference in IRAP patterns between marginal and relatively normal populations.

Molecular cytogenetic evaluation of transposable element diversity

To confirm the IRAP data on retrotransposon diversity, specifically the distribution of the Ty1-*copia* and Ty3-*gypsy* retrotransposon superfamilies within the marginal and central populations, an independent evaluation of transposable element diversity was performed. The method of comparative molecular cytogenetics, which allows for an integral evaluation of the genomic distribution of retrotransposons, was used. We applied a categorical sampling approach in which marginal populations were pairwise compared with relatively normal populations. The results are shown in Figure 5. We evaluated the total number of major blocks in the genome. The number of blocks of both the Ty1-*copia* and Ty3-*gypsy* retrotransposons was greatly reduced in marginal populations compared with normal populations. In the TS84 population, there are 34 major blocks of Ty1-*copia* (Figure 5A) and 26 major blocks of Ty3-*gypsy* (Figure 5C) elements. These blocks mostly coincided with distal/terminal clusters of heterochromatin, which are present on all chromosomes of plants from central populations of *Ae. speltoides*. In the marginal Q population, the number of blocks for both Ty1-*copia* (Figure 5B) and Ty3-*gypsy* (Figure 5D) elements was reduced to 13. The appearance of Ty3-*gypsy* intercalary block on B chromosomes was also observed. Thus, the data from the molecular cytogenetic analysis were consistent with the IRAP data in terms of the significant reconstitution of the tested retrotransposon patterns in marginal populations.

Discussion

Variability of the IRAP patterns for the WIS2, Wilma, and Daniela LTR retrotransposons

A high level of intraspecific variability in nuclear DNA LTR retrotransposon fractions of *Ae. speltoides* was revealed by IRAP analysis. This marker system appears to be an appropriate approach for the evaluation of genetic diversity and evolutionary relationships within and between species (Saeidi *et al.* 2008). Moreover, part of the changes in IRAP patterns can be attributed to recent proliferation as differences in IRAP patterns between parental genotypes and offspring in *Ae. speltoides* populations have been previously

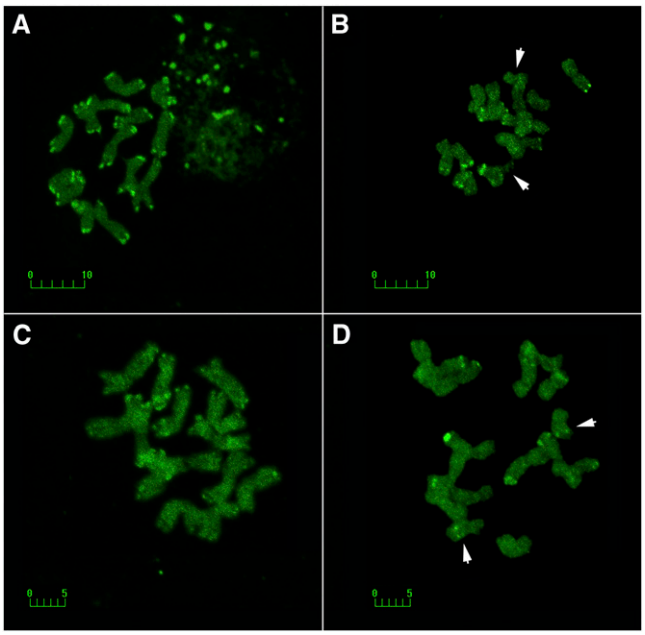

Figure 5 Molecular cytogenetic display of transposable element diversity. (A–D) Comparison of FISH signals from the Ty1-*copia* (A and B) and Ty3-*gypsy* (C and D) LTR retrotransposons in genotypes of *Ae. speltoides* from contrasting populations: the central population from Latakia (TS84) (A and C) and the marginal Kishon (Q) population (B and D). The B chromosomes are arrowed. Bars: 10 μm and 5 μm.

reported (Belyayev *et al.* 2010). Various genotypes from the same population differ substantially in the distribution patterns of the four explored LTR retrotransposons. This diversity points to a permanent ongoing process of LTR retrotransposon fractions restructuring in different populations of *Ae. speltoides* along the species' range. Despite the observed diversity, PCA of IRAP patterns for three LTR retrotransposons, *WIS2*, *Wilma*, and *Daniela*, revealed an association of the majority of individuals of each population into sufficiently dense groups (less dense for *WIS2* and more dense for *Wilma*) that often overlap (*i.e.*, possessed similar IRAP patterns; Figure 3, A–C). This is particularly emphasized by QDA analysis when misclassifications inside a single population are present, but represent only a small percentage (Figure 4, A–C). It is also essential to note that the peripheral northernmost population, C, and the southern small, marginal populations, Q and T0, T2, and T5, stand out. The most striking case is the very unusual IRAP pattern of the *Daniela* element in the Kishon population (highlighted with a yellow circle in Figure 3C). This population is extremely small (100 m^2) and has been nearly destroyed by anthropogenic factors. In addition, this is the only Israeli population that is located at sea level (2 m above) and is close to the Akko plain terminal of desert plants (Raskina *et al.* 2004b). It is likely that such an extreme environment has been a crucial factor in the changing pattern of the *Daniela* element. Although the mechanisms for this phenomenon are unclear, we speculate that it might have resulted from the high recombination rate that is typical of marginal populations (see also Raskina *et al.* 2011); even so, it is possible that a transposition also contributed to the radical changes in the IRAP pattern.

Further evidence of the permanence of LTR retrotransposon fraction repatterning was provided by time-line IRAP analysis of genotypes from the Technion 2 population, when three sets of plants collected in different years (T0, T2, and T5) were analyzed. This population is extremely small, degraded (*i.e.*, partially destroyed by nearby construction and advancing shrubs), and isolated. Moreover, due to *Ae. speltoides* cross-pollination, this population could be considered an inbred colony. Therefore, we would expect a rather uniform IRAP pattern. The latter is true for *Wilma* and *Daniela* elements, but, for *WIS2* retrotransposons, the real data are quite the opposite. Each of the analyzed generations has an individual distribution cloud, and, despite a sufficiently large overlap region, individual genotypes are at a considerable distance from each other (Figure 3A), thus showing a constant restructuring of the *WIS2* element pattern over time.

The IRAP retrotransposon display and the following statistical analysis revealed differences between the Ty3-*gypsy* (*Wilma* and *Daniela*) and Ty1-*copia* (*WIS2*) retrotransposon superfamilies (Figure 3). Some of these differences result from the structural features of these elements (Suoniemi *et al.* 1998) and their positions in the genome (Belyayev *et al.* 2001). However, apart from these differences, our data indicate that there is an important relationship between populations under great stress and high levels of both Ty3-*gypsy* and Ty1-*copia* LTR retrotransposon diversity. For example, the majority of the genotypes for the elements of both superfamilies in the Q and T0, T2, and T5 populations form a distinct cluster separated from the main group formed by the rest of the populations. This observation was confirmed by molecular cytogenetic analysis of contrasting populations, which also supported the conclusion that there is a significant difference between the patterns of Ty3-*gypsy* and Ty1-*copia* LTR retrotransposons in marginal and normal populations. In both southern and northern marginal populations, we observed a significant decrease in the number of major blocks and detected repatterning. These results are similar to those obtained for species-specific tandem repeats in marginal populations (Raskina *et al.* 2011).

Variability of the IRAP pattern for the Fatima LTR retrotransposon

Each of the investigated LTR retroelements has a unique IRAP pattern distribution (Figure 3); at the same time, the patterns of *Daniela*, *Wilma*, and *WIS2* elements resemble one other (Figures 3, A–C, and 4, A–C). Conversely, the PCA distribution of the *Fatima* element is significantly different from that of the three other LTR retroelements. QDA analysis also confirmed the special status of the *Fatima* element. The investigated populations fall into three distinct groups (Figures 3D and 4D). Group I (Figure 3D) consists of the majority of *Ae. speltoides*, *Ae. sharonensis*, and *Ae. longissima* genotypes and all genotypes of *Ae. bicornis*. The occurrence of several

species in a dense group points to the stability of the *Fatima* IRAP pattern over time. This may result from complete silencing of the element for a long period and/or from relatively short LTRs of Fatima, *i.e.*, a poor template for recombination. Anyway, violations of this pattern, such as those observed in groups II and III (Figure 3D), may indicate the movement of elements in the genome. This movement may be a movement of the element itself by a copy and paste mechanism, indicating the activity of *Fatima* elements in some genotypes, and/or it can be the rebuilding of blocks enriched with *Fatima* retrotransposons. In any case, this movement can be regarded as a significant microevolutionary event in the genome, especially if inherited.

The next important question is, What is common between genotypes with restructured *Fatima* element IRAP patterns? Obviously, 96% of these genotypes are from stressed, critically endangered micropopulations. The population of TS43 consisted of just a few plants collected in 1979, which were not found again (M. Feldman, personal communication). This is also the case for the Technion 2 population that was found by the authors in 2000, but was extinct in 2006. Genotypes of *Ae. sharonensis* (S) are from the northernmost population of Kishon, and *Ae. longissima* (L) genotypes are from the degraded coastal Wingate population (group II in Figure 3D). Nevertheless, in large populations, a small percentage of genotypes with an unusual IRAP pattern of *Fatima* elements are also present, as evidenced by *Ae. speltoides* genotypes from a large population of K. The consequences of *Fatima* element IRAP pattern rebuilding still need to be determined.

Estimation of the level of IRAP pattern variability

The material examined showed a range of changes in the IRAP pattern, so the next salient question is, How can we estimate the level of LTR retrotransposon IRAP pattern variability? In other words, What kind of information can we get from the differences in the IRAP patterns between genotypes and between populations in terms of microevolution, and how valuable is this information? The answer to these questions can be obtained by interspecific comparisons. The PCA of the three LTR retroelements, namely *WIS2*, *Daniela*, and *Wilma*, showed that *Sitopsis* species *Ae. sharonensis* and *Ae. longissima* usually form a group, while *Ae. bicornis* stands separately and in an intermediate position between this group and *Ae. speltoides* (Figure 3, A–C). The group consisting of *Ae. sharonensis* and *Ae. longissima* is located some distance from the weighted average of the plot. This distance is $>|0.1|$ for *WIS2*, $>|0.2|$ for *Wilma*, and $>|0.15|$ for *Daniela*. We might ask for which of the three elements can the corresponding distance be taken as characteristic of the species character. In the case of *WIS2* retrotransposons, the distance is meaningless because many genotypes are outside the specified values without having any deviations in *habitus*. Most likely, the large variability of *WIS2* IRAP pattern was the result of neutral heterochromatin conversions, as heterochromatin is known to be enriched with elements of the Ty1-*copia* family (Pearce *et al.* 1996; Heslop-Harrison *et al.* 1997; Belyayev *et al.* 2001; Saunders and Houben 2001; Chang *et al.* 2008). Thus, the variability of *WIS2* element IRAP patterns can only be an indicator of the intensity of genomic rearrangements.

For *Wilma* retroelements, no genotypes exceed the specified values (Figure 3B); consequently, the data for this element can be taken as a species characteristic. In the case of *Daniela* elements, nine genotypes from the Q population are at the specified distance from the majority of the *Ae. speltoides* genotypes (Figure 3C). This population is located on the western banks of the Kishon River (Haifa Bay area, Israel) and is characterized by high heteromorphy, possessing a wide spectrum of chromosomal abnormalities (Raskina *et al.* 2004a) and enhanced levels of TE proliferation (Belyayev *et al.* 2010). We assumed that intensive, ongoing intragenomic processes in this population could ultimately create the basis for parapatric speciation (Raskina *et al.* 2004b). As has been repeatedly shown, the *Daniela* retrotransposon extensively amplified during the speciation of diploid ancestors of the A and D genomes of cultivated wheat (Liu *et al.* 2008); therefore, it can be reasonably suggested that significant changes in the *Daniela* IRAP pattern may accompany the speciation process.

An analysis of relationships between Sitopsis species

IRAP analysis for *WIS2*, *Wilma*, and *Daniela* elements revealed a grouping similar to those determined by other methods, where *Ae. sharonensis* and *Ae. longissima* form a separate unit, *Ae. speltoides* appears as a dispersed group, and *Ae. bicornis* is in an intermediate position. Similar configurations were revealed by the RFLP method (Giorgi *et al.* 2002), by α-amylase inhibitor gene analysis (Wang *et al.* 2007), by sequence-specific amplification polymorphism (Queen *et al.* 2003), and on the basis of chloroplast DNA changes (Miyashita *et al.* 1994). These data suggest a very recent divergence of local endemics (*i.e.*, *Ae. sharonensis* and *Ae. longissima*) from the common progenitor. Because both species are young, genetic barriers are not yet completely formed, and interspecific hybrids are not only possible but also fertile (Ankory and Zohary 1962).

Taking all of the above lines of evidence together, the IRAP display data revealed dynamic changes of LTR retrotransposon fractions in the genome of *Ae. speltoides*. The process is permanent and population specific, ultimately leading to the separation of small stressed populations from the main group.

Acknowledgments

The authors are most grateful to Jerzy Jurka and anonymous reviewers for helpful comments. A.B. and O.R. designed the project. R.K. designed IRAP primers. E.H. performed the experiments. L.B. performed statistical analysis. A.B. and O.R. wrote the paper. This work is supported by grants from the Israel Science Foundation to A.B. and O.R. (grant 723/07).

Literature Cited

Ankory, H., and D. Zohary, 1962 Natural hybridization between *Aegilops sharonensis* and *Ae. longissima*: a morphological and cytological study. Cytologia (Tokyo) 27: 314–324.

Ansari, K. I., S. Walter, J. M. Brennan, M. Lemmens, S. Kessans *et al.*, 2007 Retrotransposon and gene activation in wheat in response to mycotoxigenic and non-mycotoxigenic-associated *Fusarium* stress. Theor. Appl. Genet. 114: 927–937.

Baucom, R. S., J. C. Estill, J. Leebens-Mack, and J. L. Bennetzen, 2009 Natural selection on gene function drives the evolution of LTR retrotransposon families in the rice genome. Genome Res. 19: 243–254.

Belyayev, A., O. Raskina, and E. Nevo, 2001 Chromosomal distribution of reverse transcriptase-containing retroelements in two *Triticeae* species. Chromosome Res. 9: 129–136.

Belyayev, A., R. Kalendar, L. Brodsky, E. Nevo, A. H. Schulman *et al.*, 2010 Transposable elements in a marginal plant population: temporal fluctuations provide new insights into genome evolution of wild diploid wheat. Mobile DNA 1: 6.

Bennetzen, J. L., 1996 The contributions of retroelements to plant genome organization, function and evolution. Trends Microbiol. 4: 347–353.

Bolstad, B. M., R. A. Irizarry, M. Astrand, and T. P. Speed, 2003 A comparison of normalization methods for high density oligonucleotide array data based on variance and bias. Bioinformatics 19: 185–193.

Brussard, P. F., 1984 Geographic patterns and environmental gradients: the Central-Marginal model in *Drosophila* revisited. Annu. Rev. Ecol. Syst. 15: 25–64.

Chang, S. B., T. J. Yang, E. Datema, J. van Vugt, B. Vosman *et al.*, 2008 FISH mapping and molecular organization of the major repetitive sequences of tomato. Chromosome Res. 16: 919–933.

Da Cunha, A. B., and T. Dobzhansky, 1954 A further study of chromosomal polymorphism in *Drosophila willistoni* in its relation to the environment. Evolution 8: 119–134.

Eckert, C. G., K. E. Samis, and S. C. Lougheed, 2008 Genetic variation across species' geographical ranges: the central–marginal hypothesis and beyond. Mol. Ecol. 17: 1170–1188.

Giorgi, D., R. D'Ovidio, A. Oronzo, O. A. Tanzarella, and E. Porceddu, 2002 RFLP analysis of *Aegilops* species belonging to the *Sitopsis* section. Genet. Resour. Crop Evol. 49: 145–151.

Grandbastien, M. A., C. Audeon, E. Bonnivard, J. M. Casacuberta, B. Chalhoub *et al.*, 2005 Stress activation and genomic impact of Tnt1 retrotransposons in Solanaceae. Cytogenet. Genome Res. 110: 229–241.

Grant, V., 1981 *Plant Speciation*, Ed. 2. Columbia University Press, New York.

Heslop-Harrison, J. S., A. Brandes, S. Taketa, T. Schmidt, V. Vershinin *et al.*, 1997 The chromosomal distributions of Ty1-copia group retrotransposable elements in higher plants and their implications for genome evolution. Genetica 100: 197–204.

Hofreiter, M., and J. Stewart, 2009 Ecological change, range fluctuations and population dynamics during the Pleistocene. Curr. Biol. 19: 584–594.

Joliffe, I. T., 2002 *Principal Component Analysis*. Springer-Verlag, Berlin/Heidelberg, Germany/New York.

Kalendar, R., and A. H. Schulman, 2006 IRAP and REMAP for retrotransposon-based genotyping and fingerprinting. Nat. Protoc. 1: 2478–2484.

Kapitonov, V. V., and J. Jurka, 2008 A universal classification of eukaryotic transposable elements implemented in Repbase. Nat. Rev. Genet. 9: 411–412.

Kashkush, K., M. Feldman, and A. A. Levy, 2003 Transcriptional activation of retrotransposons alters the expression of adjacent genes in wheat. Nat. Genet. 32: 102–106.

Kidwell, K. K., and T. C. Osborn, 1992 Simple plant DNA isolation procedures, pp. 1–13 in *Plant Genomes: Methods for Genetic and Physical Mapping*, edited by J. S. Beckmann, and T. C. Osborn Kluwer Academic Publishers, Dordrecht, Netherlands.

Kimber, G., and M. Feldman, 1987 *Wild Wheat, an Introduction*. College of Agriculture, University Missouri, Columbia, MO.

Kirkpatrick, M., and N. H. Barton, 1997 Evolution of a species' range. Am. Nat. 150: 1–23.

Kröpelin, S., D. Verschuren, A. M. Lézine, H. Eggermont, C. Cocquyt *et al.*, 2008 Climate-driven ecosystem succession in the Sahara: the past 6000 years. Science 320: 765–768.

Liu, Z., W. Yue, D. Li, R.-C. Wang, X. Kong *et al.*, 2008 Structure and dynamics of retrotransposons at wheat centromeres and pericentromeres. Chromosoma 117: 445–456.

Martienssen, R., 2008 Great leap forward? Transposable elements, small interfering RNA and adaptive Lamarckian evolution. New Phytol. 179: 572–574.

Mayr, E., 1963 *Animal Species and Evolution*. Belknap Press, Cambridge, MA.

Mayr, E., 1970 *Populations Species and Evolution. An Abridgment of Animal Species and Evolution*, Belknap Press, Cambridge, MA.

Miyashita, N. T., N. Mont, and K. Tsunewaki, 1994 Molecular variation in chloroplast DNA regions in ancestral species of wheat. Genetics 137: 883–889.

Pearce, S. R., U. Pich, G. Harrison, A. J. Flavell, J. S. Heslop-Harrison *et al.*, 1996 The Ty1-*copia* group retrotransposons of *Allium cepa* are distributed throughout the chromosomes but are enriched in the terminal heterochromatin. Chromosome Res. 4: 357–364.

Press, W. H., B. P. Flannery, S. A. Teukolsky, and W. T. Vetterling, 2007 *Numerical Recipes*. Cambridge University Press, Cambridge, UK.

Purugganan, M. D., and S. R. Wessler, 1994 Molecular evolution of *magellan*, a maize Ty3/*Ty3-gypsy*-like retrotransposon. Proc. Natl. Acad. Sci. USA 91: 11674–11678.

Queen, R. A., B. M. Gribbon, C. James, P. Jack, and A. J. Flavell, 2003 Retrotransposon-based molecular markers for linkage and genetic diversity analysis in wheat. Mol Gen. Genomics 271: 91–97.

Raskina, O., A. Belyayev, and E. Nevo, 2004a Activity of the *En/Spm*-like transposons in meiosis as a base for chromosome repatterning in a small, isolated, peripheral population of *Aegilops speltoides* Tausch. Chromosome Res. 12: 153–161.

Raskina, O., A. Belyayev, and E. Nevo, 2004b Quantum speciation in *Aegilops*: molecular cytogenetic evidence from rDNA cluster variability in natural populations. Proc. Natl. Acad. Sci. USA 101: 14818–14823.

Raskina, O., L. Brodsky, and A. Belyayev, 2011 Tandem repeats on an eco-geographical scale: outcomes from the genome of *Aegilops speltoides*. Chromosome Res. 19: 607–623.

Rebernig, C. A., H. Weiss-Schneeweiss, G. M. Schneeweiss, P. Schönswetter, R. Obermayer *et al.*, 2010 Quaternary range dynamics and polyploid evolution in an arid brushland plant species (*Melampodium cinereum*, *Asteraceae*). Mol. Phylogenet. Evol. 54: 594–606.

Saeidi, H., M. R. Rahiminejad, and J. S. Heslop-Harrison, 2008 Retroelement insertional polymorphisms, diversity and phylogeography within diploid, D-genome *Aegilops tauschii* (*Triticeae*, *Poaceae*) sub-taxa in Iran. Ann. Bot. (Lond.) 101: 855–861.

Saunders, V. A., and A. Houben, 2001 The pericentromeric heterochromatin of the grass *Zingeria biebersteiniana* (2n = 4) is composed of Zbcen1-type tandem repeats that are intermingled with accumulated dispersedly organized sequences. Genome 44: 955–961.

Suoniemi, A., J. Tanskanen, and A. H. Schulman, 1998 Gypsy-like retrotransposons are widespread in the plant kingdom. Plant J. 13: 699–705.

Tchernov, E., 1988 The biogeographical history of southern Levant, pp. 159–251 in *The Zoogeography of Israel: The Distribution and Abundance at a Zoogeographical Crossroad*, edited by Y. Yom-Tov, and E. Tchernov. Dr. W. Junk Publishers, Kluwer Academic Publishers, Dordrecht, Netherlands.

Tsukahara, S., A. Kobayashi, A. Kawabe, O. Mathieu, A. Miura *et al.*, 2009 Bursts of retrotransposition reproduced in Arabidopsis. Nature 461: 423–426.

VanderWiel, P. L., D. F. Voytas, and J. F. Wendel, 1993 *Ty1-copia*-like retrotransposable element evolution in diploid and polyploid cotton (*Gossypium* L.). J. Mol. Evol. 36: 429–447.

Vitte, C., and O. Panaud, 2003 Formation of solo-LTRs through unequal homologous recombination counterbalances amplifications of LTR retrotransposons in rice *Oryza sativa* L. Mol. Biol. Evol. 20: 528–540.

Wang, J.-R., L. Zhang, Y.-M. Wei, Z.-H. Yan, B. R. Baum *et al.*, 2007 Sequence polymorphisms and relationships of dimeric a-amylase inhibitor genes in the B genomes of *Triticum* and S genomes of *Aegilops*. Plant Sci. 173: 1–11.

Wessler, S. R., 1996 Turned on by stress. Plant retrotransposons. Curr. Biol. 6: 959–961.

Wicker, T., N. Yahiaoui, R. Guyot, E. Schlagenhauf, Z. D. Liu *et al.*, 2003 Rapid genome divergence at orthologous low molecular weight glutenin loci of the A and Am genomes of wheat. Plant Cell 15: 1186–1197.

Zohary, D., J. R. Harlan, and A. Vardi, 1969 The wild diploid progenitors of wheat and their breeding value. Euphytica 18: 58–65.

Communicating editor: D. Voytas

GENETICS

Supporting Information
http://www.genetics.org/content/suppl/2011/10/31/genetics.111.134643.DC1

Diversity of Long Terminal Repeat Retrotransposon Genome Distribution in Natural Populations of the Wild Diploid Wheat *Aegilops speltoides*

Elena Hosid, Leonid Brodsky, Ruslan Kalendar, Olga Raskina, and Alexander Belyayev

DOI: 10.1534/genetics.111.134643

Table S1 Characteristics of *Ae. speltoides* populations

Abbreviation of population	Populations: origin, source	Geographical zone, elevation, and coordinates	Population size, location	Morphotype
C	Cankiri, Turkey[4] PI 573448	Euro-Siberian 680 m 40º31' N, 33º38' E	N/A; cultivated field *	ssp. *ligustica*
An	Ankara, Turkey[1] PI 573452	Irano-Turanian 575 m 36º59' N, 32º56' E	N/A; cultivated field *	ssp. *ligustica*
Ar	Arbil, Iraq[1] PI 219867	Irano-Turanian 570 m 36º24' N, 44º08' E	N/A; uncultivated area *	ssp. *ligustica*
TS-84	Latakia, Syria[3,4] PI 487235, TS-84	Mediterranean 200 m 35º38' N, 35º59' E	N/A; uncultivated area *	ssp. *aucheri*
Ta	Tartus, Syria[1] PI 487238	Mediterranean 600 m 35º07' N, 36º07' E	N/A; cultivated field *	ssp. *aucheri*
A	Achihood, Israel[4] 2.16	Mediterranean 45-75 m 32º55' N, 35º10' E	big; cultivated field and natural habitat	ssp. *ligustica* ssp. *aucheri*
E	En-Efek, Israel[4] 2.37	Mediterranean 16 m 32º50' N, 35º06' E	small; uncultivated area; endangered	ssp. *ligustica*

Q	Kishon, Israel[4]	Mediterranean	small;	ssp. *ligustica*
	2.22	2 m	natural habitat	ssp. *aucheri*
		32º48' N; 35º02' E	endangered	
T0, T2, T5	Technion-2, Israel[4]	Mediterranean	small;	ssp. *ligustica,*
	2.36	265 m	natural abitat;	ssp. *aucheri*
		32º46' N, 35º00' E	extinct	
R	Ramat Hanadiv, Israel[4]	Mediterranean	big;	ssp. *ligustica,*
	2.46	100-125 m	natural habitat, interrupted area	ssp. *aucheri,*
		32º33' N, 34º56' E		*intermediate*
K	Katzir, Israel[3; 4]	Mediterranean	big;	ssp. *aucheri*
	TS 89	233-250 m	natural habitat	
		32º29' N, 35º05' E		
TS 43	Givat Koah, Israel[4]	Mediterranean	small;	intermediate
	TS 43	75 m	uncultivated area;	
		32º02' N, 34º58' E *	extinct	
TS 01	Ashkelon, Israel[3]	Mediterranean	N/A;	ssp. *aucheri*
	TS 01	45 m	uncultivated area,	
		31º40' N, 34º38' E *	extinct	

Source: [1] – USDA, United States Department of Agriculture; [2] – AARI, Aegean Agricultural Research Institute, Turkey; [3] – kindly provided by Prof. M. Feldman, Weizmann Institute collection, Rehovot, Israel; [4] – IE, Institute of Evolution collection, Haifa, Israel; * - data obtained by Google Earth.

Table S2 All IRAP primers produced multiple fragments from genomic DNA of all *Ae. speltoides*, *Ae. sharonensis, Ae. longissima,* and *Ae. bicornis* accessions

Table S2 is available for download as an Excel file at http://www.genetics.org/content/suppl/2011/10/31/genetics.111.134643.DC1.